

Entanglement Swapping and Quantum Correlations via Symmetric Joint Measurements

Cen-Xiao Huang^{1,2,3,*} Xiao-Min Hu,^{1,2,3,*} Yu Guo^{1,2,3} Chao Zhang^{1,2,3} Bi-Heng Liu,^{1,2,3,†} Yun-Feng Huang,^{1,2,3} Chuan-Feng Li,^{1,2,3,‡} Guang-Can Guo,^{1,2,3} Nicolas Gisin^{4,5} Cyril Branciard⁶ and Armin Tavakoli^{7,8,§}

¹CAS Key Laboratory of Quantum Information, University of Science and Technology of China, Hefei 230026, China

²CAS Center For Excellence in Quantum Information and Quantum Physics,
University of Science and Technology of China, Hefei 230026, China

³Hefei National Laboratory, University of Science and Technology of China, Hefei 230088, China

⁴Group of Applied Physics, University of Geneva, 1211 Geneva 4, Switzerland

⁵Schaffhausen Institute of Technology—SIT, 1211 Geneva, Switzerland

⁶Université Grenoble Alpes, CNRS, Grenoble INP, Institut Néel, 38000 Grenoble, France

⁷Institute for Quantum Optics and Quantum Information—IQOQI Vienna, Austrian Academy of Sciences,
Boltzmannsgasse 3, 1090 Vienna, Austria

⁸Atominstitut, Technische Universität Wien, Stadionallee 2, 1020 Vienna, Austria



(Received 30 March 2022; accepted 17 June 2022; published 13 July 2022)

We use hyperentanglement to experimentally realize deterministic entanglement swapping based on quantum elegant joint measurements. These are joint projections of two qubits onto highly symmetric, isoentangled bases. We report measurement fidelities no smaller than 97.4%. We showcase the applications of these measurements by using the entanglement swapping procedure to demonstrate quantum correlations in the form of proof-of-principle violations of both bilocal Bell inequalities and more stringent correlation criteria corresponding to full network nonlocality. Our results are a foray into entangled measurements and nonlocality beyond the paradigmatic Bell state measurement and they show the relevance of more general measurements in entanglement swapping scenarios.

DOI: [10.1103/PhysRevLett.129.030502](https://doi.org/10.1103/PhysRevLett.129.030502)

Introduction.—Entangled measurements, i.e., projections of several qubits onto a basis of entangled states, are an indispensable resource for quantum information processing. They are crucial for paradigmatic protocols such as teleportation [1], dense coding [2], entanglement swapping [3], and quantum repeaters [4,5], as well as for emerging topics such as network nonlocality [6] and entanglement-assisted quantum communications [7,8].

However, while entangled states have been broadly researched [9], the complementary case of entangled measurements has been largely focused on the paradigmatic Bell state measurement, i.e., the projection of (say) two qubits onto the four maximally entangled states $|\phi^\pm\rangle = (1/\sqrt{2})(|00\rangle \pm |11\rangle)$ and $|\psi^\pm\rangle = (1/\sqrt{2})(|01\rangle \pm |10\rangle)$. This measurement has been experimentally realized in a variety of contexts within the broader area of entanglement swapping and quantum correlations (see, e.g., Refs. [10–20]). Presently, not much is known about the foundational relevance, practical implementation, and overall usefulness of more general entangled measurements.

Recently, a class of entangled 2-qubit measurements has been proposed that is qualitatively different from the Bell state measurement. It displays elegant and natural symmetries and it is gaining an increasingly relevant role as a quantum information resource. These so-called elegant joint measurements (EJMs) are composed of a basis of

isoentangled states with the property that if either qubit is lost, the four possible remaining single-qubit states form a regular tetrahedron inside the Bloch sphere. Although originally introduced in the context of collective spin measurements [21,22], they were reintroduced in order to remedy the shortcomings of the Bell state measurement in triangle nonlocality [23] and were later found relevant for quantum state discrimination [24]. Very recently, they have been used as the central component of both network nonlocality protocols, which bear no resemblance to standard Bell inequality violations [25], and full network nonlocality protocols, which constitute a stronger, more genuine notion of network nonlocality [26]. The progress has also motivated recent experiments that realize one type of EJM on a superconducting quantum processor [27] and as a photonic quantum walk [28,29].

Here, we go beyond the Bell state measurement and experimentally demonstrate entanglement swapping and quantum correlations based on the EJMs. We use hyperentanglement between the polarization and path degrees of freedom in a pair of photons to create two pairs of maximally entangled states. Then, we realize a generic quantum circuit for implementing any EJM and report high-fidelity entanglement swapping. We leverage this for tests of quantum correlations in entanglement swapping scenarios, originally developed in [25,26], that for the first

time are not based on the Bell state measurement. These tests, which may be viewed as proof-of-principle tests of quantum networks, are centered about the initial independence of the two entangled pairs.

Theoretical background.—An EJM, labeled by a parameter $\theta \in [0, (\pi/2)]$, is a projection onto the following basis of a 2-qubit Hilbert space [25]:

$$\begin{aligned} |\psi_{+++}^\theta\rangle &= \frac{1}{2}(e^{-\frac{i\theta}{4}}|00\rangle - r_+^\theta|01\rangle - r_-^\theta|10\rangle + e^{-\frac{3i\theta}{4}}|11\rangle), \\ |\psi_{+--}^\theta\rangle &= \frac{1}{2}(e^{\frac{i\theta}{4}}|00\rangle + r_-^\theta|01\rangle + r_+^\theta|10\rangle + e^{\frac{3i\theta}{4}}|11\rangle), \\ |\psi_{-+-}^\theta\rangle &= \frac{1}{2}(e^{-\frac{3i\theta}{4}}|00\rangle + r_-^\theta|01\rangle + r_+^\theta|10\rangle + e^{-\frac{i\theta}{4}}|11\rangle), \\ |\psi_{--+}^\theta\rangle &= \frac{1}{2}(e^{\frac{3i\theta}{4}}|00\rangle - r_+^\theta|01\rangle - r_-^\theta|10\rangle + e^{\frac{i\theta}{4}}|11\rangle), \end{aligned} \quad (1)$$

where $r_\pm^\theta = [(1 \pm e^{i\theta})/\sqrt{2}]$. We denote the four possible outcomes of the measurement (indicated as the states' subscripts) by a string of three bits $b = (b^1, b^2, b^3) \in \{+1, -1\}^3$ such that $b^1 b^2 b^3 = 1$. The elegant property of these measurements is that all basis states are equally entangled and that the two sets of four reduced states, when the right or left qubit is lost, respectively, form two mirror-image regular tetrahedra of radius $(\sqrt{3}/2)\cos\theta$ inside the Bloch sphere, whose vertices are parallel and antiparallel with the Bloch sphere direction (b^1, b^2, b^3) , respectively. Notably, for $\theta = (\pi/2)$, the EJM is equivalent to the Bell state measurement up to local unitaries.

We apply the EJM for entanglement swapping. Consider that qubits B_1 and B_2 in the two, initially independent, maximally entangled states $|\phi^+\rangle_{AB_1} \otimes |\phi^+\rangle_{B_2C}$ are subjected to the EJM. This produces the output b with probability $p(b) = \frac{1}{4}$ and stochastically renders qubits A and C in one of the four isoentangled states (up to complex conjugation). Consider now that the qubits A and C can each be independently measured with the three Pauli observables (sometimes up to a sign), specifically $-\sigma_x$, σ_y , and $-\sigma_z$. For qubit A (C) we associate these with inputs labeled $x \in \{1, 2, 3\}$ ($z \in \{1, 2, 3\}$) and label the outputs $a \in \{\pm 1\}$ ($c \in \{\pm 1\}$). Examining the correlators between the three measurement events, one finds that $\langle A_x B^y C_z \rangle = -[1 + (-1)^\sigma \sin\theta]/2$, where $\sigma = 0$ ($\sigma = 1$) if (x, y, z) is an even (odd) permutation of $(1, 2, 3)$, and $\langle A_x B^y C_z \rangle = 0$ otherwise. Moreover, the two-body correlators are $\langle A_x B^y \rangle = -(\cos\theta/2)\delta_{x,y}$, $\langle B^y C_z \rangle = (\cos\theta/2)\delta_{y,z}$, and $\langle A_x C_z \rangle = 0$, and the one-body correlators all vanish. Here, the correlators are defined as $\langle A_x B^y C_z \rangle = \sum_{a,b,c} ab^y c p(a, b, c|x, z)$ and analogously for the two- and one-body cases.

We can think of these correlations as arising in the simplest quantum network. In general, a quantum network consists of a number of parties that are connected to each other, in some configuration, via multiple independent

sources that distribute entangled states. They are natural generalizations of the standard Bell scenario, which features only a single source connecting all parties. Correlations observed in such scenarios are called network nonlocal if they cannot be modeled by associating an independent local variable to each source. This independence is the crucial feature that takes network nonlocality conceptually beyond standard Bell nonlocality (see, e.g., Refs. [30–35]). In our scenario, called the bilocal scenario, a network local model reads $p(a, b, c|x, z) = \int d\lambda d\mu q_\lambda^{(1)} q_\mu^{(2)} p(a|x, \lambda) p(b|\lambda, \mu) p(c|z, \mu)$ for some local variable densities $q_\lambda^{(1)}$ and $q_\mu^{(2)}$.

Reference [25] showed that the above quantum correlations are nonbilocal; i.e., we cannot assign local variables to systems AB_1 and B_2C , respectively. This is witnessed through the violation of the bilocal Bell inequality

$$\mathcal{B} \equiv \frac{S}{3} - T \leq 3 + f(Z), \quad (2)$$

where $S = \sum_{k=1}^3 (\langle B^k C_k \rangle - \langle A_k B^k \rangle)$, $T = \sum_{x \neq y \neq z \neq x} \langle A_x B^y C_z \rangle$, and $Z = \max(\mathcal{C})$, where $\mathcal{C} = \{|\langle A_1 \rangle|, \dots, |\langle A_3 B^3 C_3 \rangle|\}$ is the list of the absolute value of all correlators that do not appear in the definitions of S or T . The term $f(Z)$ is a correction term relevant to the experimental reality that measured correlators in \mathcal{C} will not equal zero. In the Supplemental Material [36], we numerically show that $f(Z) = Z + 4Z^2$ is a valid correction term as long as $Z \lesssim 0.55$. The quantum protocol achieves $\mathcal{B} = 3 + \cos\theta$, which for an ideal implementation ($Z = 0$) gives a violation for every EJM except the Bell state measurement ($\theta = (\pi/2)$). The latter is merely a feature of our quantum protocol. In contrast to many other criteria for network nonlocality, which are tailored for employing the Bell state measurement (see, e.g., Refs. [30, 31, 37–40]), our quantum protocol and bilocal Bell inequality are not based on using standard Bell nonlocality as a building block for network nonlocality.

The quantum correlations also reveal stronger forms of network nonlocality. Reference [26] introduced the concept of full network nonlocality. Again assuming only the initial independence of systems AB_1 and B_2C , the correlations are said to be full network nonlocal if they cannot be modeled by any theory in which one source corresponds to a local variable and the other to a generalized, perhaps even postquantum, nonlocal resource. Notably, many known network Bell inequalities, tailored for the Bell state measurement, fail to reveal full network nonlocality [6].

However, the EJMs enable a successful detection. Full network nonlocality is implied by the simultaneous violation of both the following inequalities [26]:

$$\begin{aligned} \mathcal{F}_1 &= -\langle A_1 B^2 C_3 \rangle - \langle A_2 B^2 \rangle \\ &+ \langle C_3 \rangle [\langle A_1 B^2 \rangle + \langle A_2 B^2 C_3 \rangle + \langle C_3 \rangle] \leq 1, \end{aligned} \quad (3)$$

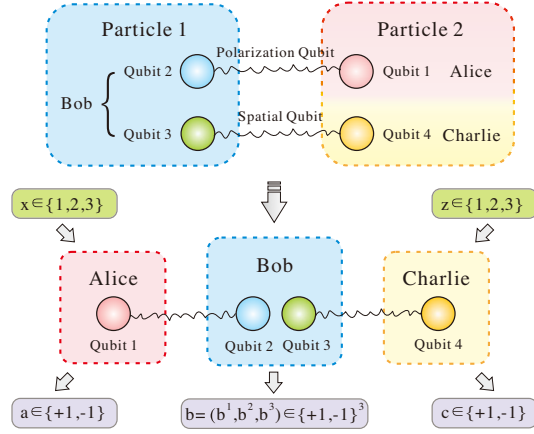


FIG. 1. Schematic diagram. Particles 1 and 2 are in a hyperentangled state $|\phi\rangle = |\phi_p^+\rangle_{12} \otimes |\phi_s^+\rangle_{34}$ of polarization qubits (p) and spatial qubits (s). The EJM is performed on qubits 2 and 3, while Pauli observables are independently performed on qubits 1 and 4, respectively.

$$\mathcal{F}_2 = -\langle A_1 B^2 C_3 \rangle + \langle B^2 C_2 \rangle + \langle A_1 \rangle [\langle B^2 C_3 \rangle - \langle A_1 B^2 C_2 \rangle + \langle A_1 \rangle] \leq 1. \quad (4)$$

The given quantum protocol achieves $\mathcal{F}_1 = \mathcal{F}_2 = \frac{1}{2}(1 + \sin \theta + \cos \theta)$, which is a violation for every $\theta \in [0, (\pi/2)]$. The largest violations are obtained for an intermediate member of the EJM family, namely, $\theta = (\pi/4)$. Notice that these violations are achieved using effectively only a binarized version of the EJM, as only Bob's outcome B^2 appears in the inequalities above. Interestingly, and in contrast to the Bell state measurement, it remains entangled even after binarization.

Experimental setup.—Our approach to experimentally realize the EJM and the associated tests of quantum correlations is represented in Fig. 1. A central fact is that, in linear optics, EJMs cannot be realized without auxiliary particles when each qubit is encoded onto a different photon [41–43]. Our approach is therefore to circumvent this issue by using two different degrees of freedom, path and polarization, of the same photon.

We generate pairs of hyperentangled states $|\phi\rangle = |\phi_p^+\rangle_{12} \otimes |\phi_s^+\rangle_{34}$. Here, $|\phi_p^+\rangle_{12} = (1/\sqrt{2})(|H\rangle|H\rangle + |V\rangle|V\rangle)$ is a polarization Bell state of qubits 1 and 2, and $|\phi_s^+\rangle_{34} = (1/\sqrt{2})(|s_0\rangle|s_0\rangle + |s_1\rangle|s_1\rangle)$ is a spatial mode Bell state of qubits 3 and 4. Using the first beam displacer (BD), we split the pump laser (775 nm) to two spatial modes (s_0 and s_1) and generate a polarization-entangled photon pair in each mode via a type-II cut periodically poled potassium titanyl phosphate (PPKTP) crystal [see Fig. 2(a)]. The hyperentanglement $|\phi\rangle = |\phi_p^+\rangle_{12} \otimes |\phi_s^+\rangle_{34}$ is obtained by tuning the relative phase between the two spatial modes [44,45]. The small separation (4 mm) of BD ensures the phase

stability [46]. We used 90 mW pumped light to excite about 2000 photon pairs per second. The coincidences to singles ratio of the entanglement source is 19%. Qubits 1 and 2 (3 and 4) are encoded in the polarization and path degrees of freedom of particle 1 (2). Attributing qubit 1 (4) to Alice (Charlie) and qubits 2 and 3 to Bob, we can rewrite the prepared state as $|\phi\rangle = |\phi^+\rangle_{AB_1} \otimes |\phi^+\rangle_{B_2C}$.

A deterministic EJM is implemented on qubits 2 (polarization) and 3 (spatial mode) following the quantum circuit proposed in Ref. [25], see Fig. 2(d). It requires controlled NOT (CNOT), C -phase, phase, and Hadamard operations [Fig. 2(e)]. By choosing qubit 3 as the control and qubit 2 as the target, the controlled gates can be realized with polarization manipulation in the different paths (see the Supplemental Material [36] for details). The CNOT gate is combined with the conversion part and is realized by using HWPs on the two paths s_0 and s_1 . A similar C -phase gate is realized by a liquid crystal phase plate. Loading different voltages on the liquid crystal produces different phases between horizontally (H) polarized light and vertically (V) polarized light. Only for path s_1 we change the phase between H and V , in order to realize the C -phase gate. We use the liquid phase crystal to load $\pi/2$ phase on H and V to complete the $\pi/2$ phase gate on the polarization qubit. We realize the phase gate and Hadamard gate by converting the path qubit into a polarization qubit. By cascading these gate operations, we realize the EJM on polarization and path qubits of a single photon. Finally, we check for correlations between the initially independent polarization and path qubits, 1 and 4, by measuring $\{\sigma_X, \sigma_Y, \sigma_Z\}$ on both sides [see Figs. 2(b) and 2(c)].

Experimental results.—We have implemented eight different choices of the EJM parameter $\theta \in \{0, (\pi/12), (\pi/6), (\pi/4), (\pi/3), (5\pi/12), (\pi/2)\}$. We reconstruct our quantum measurement from the obtained data via measurement tomography following the maximum-likelihood method [47]. In particular, we record a measurement fidelity of $98.5\% \pm 0.1\%$ for $\theta = 0$ and $97.5\% \pm 0.2\%$ for $\theta = (\pi/4)$. Details are provided in the Supplemental Material [36]. Moreover, we have measured the fidelity of our entanglement swapping procedure through the fidelity between the EJM eigenstates and the postmeasurement state of system AC . For the two most relevant cases, namely, $\theta = 0$ and $\theta = (\pi/4)$, the average fidelity of the swapped state is $98.5\% \pm 0.2\%$ and $97.5\% \pm 0.2\%$, respectively.

For each of the chosen values of θ , we have tested the bilocal Bell inequality (2) and the criterion (3) and (4) for full network nonlocality. For each setting (x, z) we measure for 10 s, recording approximately 20 000 coincidences. We observe correlations strong enough to demonstrate both nonbilocality and full network nonlocality. For the former, we obtain the largest violation by implementing the EJM at $\theta = 0$, measuring $\mathcal{B} = 3.922 \pm 0.018$, while the right-hand side of inequality (2) (its bilocal bound) is 3.092 ± 0.012 . For the latter, we obtain at best $\mathcal{F}_1 = 1.112 \pm 0.006$ and

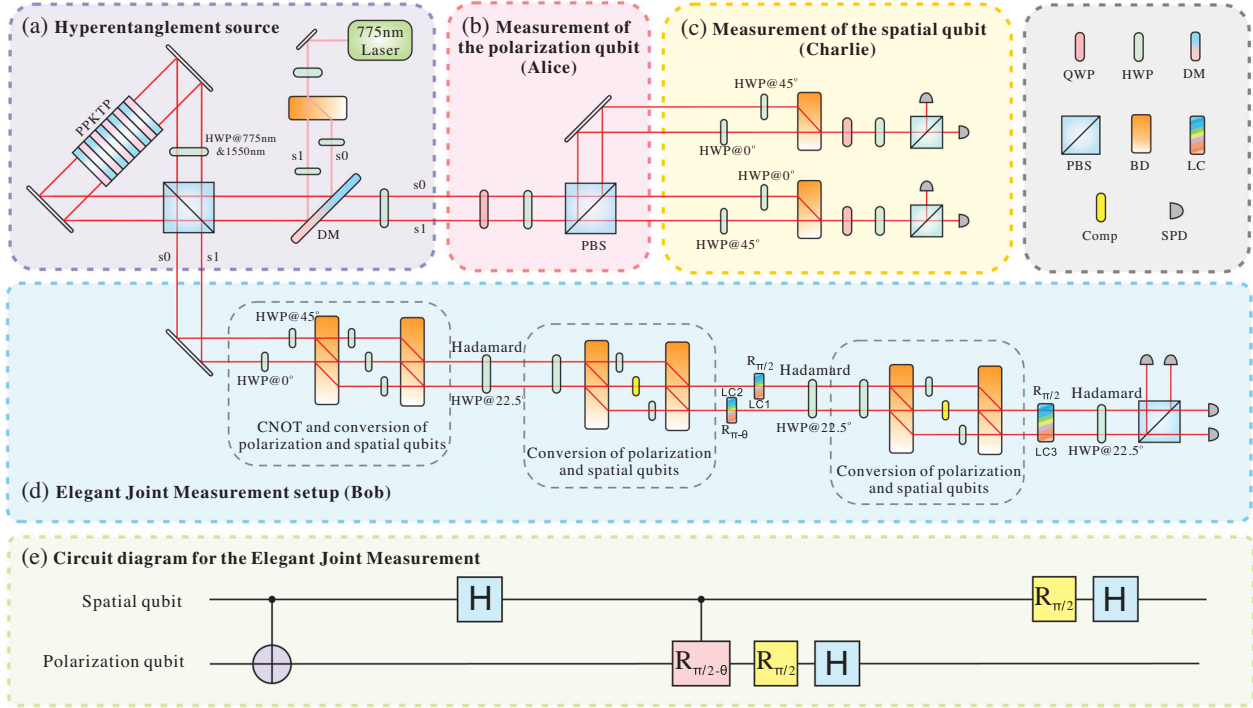


FIG. 2. Experimental setup. (a) Preparation of the hyperentangled states $\frac{1}{2}(|H\rangle|H\rangle + |V\rangle|V\rangle) \otimes (|s_0\rangle|s_0\rangle + |s_1\rangle|s_1\rangle)$. (b) Alice's measurement of the polarization qubit: settings $\{\sigma_X, \sigma_Y, \sigma_Z\}$ are implemented via quarter and half wave plates (QWPs, HWPs). (c) Charlie's measurement of the spatial qubit (first converting it into polarization). (d) Bob's EJM setup. We use different optical elements on the two paths (combined appropriately with the subsequent polarization-to-spatial conversion setup; see details in the Supplemental Material [36]) to realize the CNOT gate. The Hadamard operation on the spatial qubit is realized by a HWP set at 22.5° , between two polarization-to-spatial conversion setups. Then two liquid crystals (LCs) in the different paths and a HWP at 22.5° are used to realize the C phase, $(\pi/2)$ phase, and Hadamard gates on the polarization qubit, where the voltage of LC1 (LC2) is set so that it realizes $R_{(\pi/2)}$ ($R_{\pi-\theta} = R_{(\pi/2)-\theta}R_{(\pi/2)}$, respectively) with $R_\phi = \begin{pmatrix} 1 & 0 \\ 0 & e^{i\phi} \end{pmatrix}$. Finally, we convert the spatial qubit to a polarization qubit again and use LC3 and HWP to realize the $(\pi/2)$ phase and Hadamard gates on the spatial (turned into polarization) qubit. (e) Circuit diagram for the EJM [25]. DM, dichroic mirror; PBS, polarization beam splitter; Comp, compensator; SPD, single photon detector.

$\mathcal{F}_2 = 1.208 \pm 0.006$ by choosing $\theta = (\pi/4)$. We note that our data for $\theta = 0$ also provide a violation of the second bilocal Bell inequality originally proposed in Ref. [25],

specifically achieving $\mathcal{B}' = 29.333 \pm 0.019$, which exceeds the bilocal bound of 28.531 (see the Supplemental Material [36] for details).

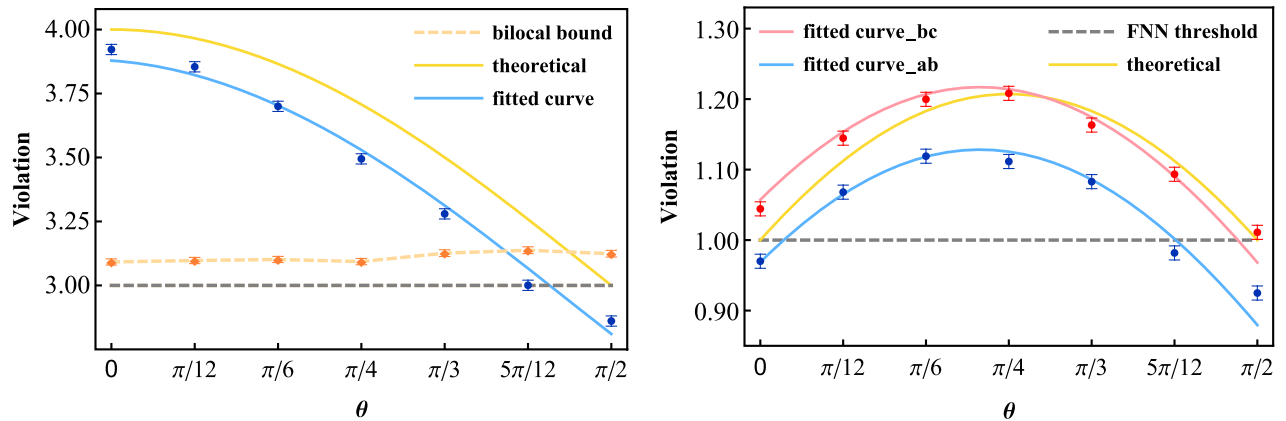


FIG. 3. Experimental results. Left: results for our test of the bilocal Bell inequality (2). The yellow curve is the theoretical prediction for the quantum correlations under consideration. The blue points are the experimental data and the blue line is a fitted curve. The orange diamonds are the bilocal bounds after consideration of the Z -correction term. Right: results for our test of full network nonlocality (FNN), via inequalities (3) and (4). The yellow curve is the theoretical prediction. The blue and red points are the experimentally measured values corresponding to \mathcal{F}_1 and \mathcal{F}_2 , respectively. The errors were estimated assuming Poissonian statistics.

Our complete correlation results are illustrated in Fig. 3. For the bilocality test, we measured $Z = 0.071 \pm 0.008$ for the most interesting case of $\theta = 0$ and at most $Z = 0.099 \pm 0.008$ over all θ . Taking into account the Z -dependent correction to the bilocal bound in (2), we record a violation for the first five values of θ . In addition, we observe full network nonlocality for four different choices of θ . Although the theory predicts $\mathcal{F}_1 = \mathcal{F}_2$, we consistently find that \mathcal{F}_2 is significantly larger than \mathcal{F}_1 . This is attributed to the phase error in the EJM setup. As discussed in the Supplemental Material [36], a small amount of such error induces a considerable offset in the values of \mathcal{F}_1 and \mathcal{F}_2 .

These correlation tests are based on the assumption of independent entangled pairs. To reasonably meet this assumption, we have carefully calibrated our setup in order to eliminate potential correlations between the initial system AB_1 and B_2C . To estimate the accuracy of the state preparation, we have, via state tomography [48], reconstructed the total state and found that it has a fidelity of $99.0\% \pm 0.1\%$ with the target state $|\phi^+\rangle_{AB_1} \otimes |\phi^+\rangle_{B_2C}$. To estimate the correlations between the two joint systems, we have evaluated both the fidelity and the quantum mutual information [49] between the tomographic reconstruction and the product of its reductions to systems AB_1 and B_2C . We obtain $99.1\% \pm 0.1\%$ and 0.048 ± 0.003 bits, respectively.

Discussion.—Our Letter constitutes a first step toward the experimental realization of entanglement swapping protocols beyond the celebrated Bell state measurement, and our experiments showcase their advantages. On the conceptual side, it is interesting to further understand the role of more general entangled measurements in quantum information processing. Already conceptualizing the extension of the EJM to multipartite settings appears to not be straightforward. On the technological side, a natural next step is to investigate entanglement swapping tests based on EJMs where all qubits are assigned separate optical carriers, i.e., with the help of auxiliary particles or nonlinear optical processes. This would enable the use of deterministic and complete EJMs in proper quantum networks. Also, provided appropriate theoretical advances take place (see, e.g., Ref. [50]), it may be interesting to extend our hyperentanglement-based approach toward proof-of-principle demonstrations of triangle-nonlocal correlations via EJMs [23].

This work was supported by the National Key Research and Development Program of China (2021YFE0113100 and 2017YFA0304100), the National Natural Science Foundation of China (11874345, 11821404, 11904357, 12174367, and 12175106), Innovation Program for Quantum Science and Technology (No. 2021ZD0301200), the Fundamental Research Funds for the Central Universities, USTC Tang Scholarship, Science and Technological Fund of Anhui Province for Outstanding Youth (2008085J02), China Postdoctoral Science Foundation (2021M700138), and China Postdoctoral for

Innovative Talents (BX2021289). A. T. was supported by the Wenner-Gren Foundations. N. G. was supported by the Swiss National Science Foundation via the National Centres of Competence in Research (NCCR)-SwissMap.

*C.-X. H. and X.-M. H. contributed equally to this work.

[†]bhliu@ustc.edu.cn

[‡]cfl@ustc.edu.cn

[§]armin.tavakoli@oeaw.ac.at

- [1] C. H. Bennett, G. Brassard, C. Crépeau, R. Jozsa, A. Peres, and W. K. Wootters, Teleporting an Unknown Quantum State via Dual Classical and Einstein-Podolsky-Rosen Channels, *Phys. Rev. Lett.* **70**, 1895 (1993).
- [2] C. H. Bennett and S. J. Wiesner, Communication via One- and Two-Particle Operators on Einstein-Podolsky-Rosen States, *Phys. Rev. Lett.* **69**, 2881 (1992).
- [3] M. Żukowski, A. Zeilinger, M. A. Horne, and A. K. Ekert, “Event-Ready-Detectors” Bell Experiment via Entanglement Swapping, *Phys. Rev. Lett.* **71**, 4287 (1993).
- [4] H.-J. Briegel, W. Dür, J. I. Cirac, and P. Zoller, Quantum Repeaters: The Role of Imperfect Local Operations in Quantum Communication, *Phys. Rev. Lett.* **81**, 5932 (1998).
- [5] L.-M. Duan, M. D. Lukin, J. I. Cirac, and P. Zoller, Long-distance quantum communication with atomic ensembles and linear optics, *Nature (London)* **414**, 413 (2001).
- [6] A. Tavakoli, A. Pozas-Kerstjens, M.-X. Luo, and M.-O. Renou, Bell nonlocality in networks, *Rep. Prog. Phys.* **85**, 056001 (2022).
- [7] A. Tavakoli, J. Pauwels, E. Woodhead, and S. Pironio, Correlations in entanglement-assisted prepare-and-measure scenarios, *PRX Quantum* **2**, 040357 (2021).
- [8] J. Pauwels, A. Tavakoli, E. Woodhead, and S. Pironio, Entanglement in prepare-and-measure scenarios: Many questions, a few answers, *New J. Phys.* **24**, 063015 (2022).
- [9] R. Horodecki, P. Horodecki, M. Horodecki, and K. Horodecki, Quantum entanglement, *Rev. Mod. Phys.* **81**, 865 (2009).
- [10] D. Boschi, S. Branca, F. De Martini, L. Hardy, and S. Popescu, Experimental Realization of Teleporting an Unknown Pure Quantum State via Dual Classical and Einstein-Podolsky-Rosen Channels, *Phys. Rev. Lett.* **80**, 1121 (1998).
- [11] J.-W. Pan, D. Bouwmeester, H. Weinfurter, and A. Zeilinger, Experimental Entanglement Swapping: Entangling Photons That Never Interacted, *Phys. Rev. Lett.* **80**, 3891 (1998).
- [12] T. Jennewein, G. Weihs, J.-W. Pan, and A. Zeilinger, Experimental Nonlocality Proof of Quantum Teleportation and Entanglement Swapping, *Phys. Rev. Lett.* **88**, 017903 (2001).
- [13] T. Yang, Q. Zhang, T.-Y. Chen, S. Lu, J. Yin, J.-W. Pan, Z.-Y. Wei, J.-R. Tian, and J. Zhang, Experimental Synchronization of Independent Entangled Photon Sources, *Phys. Rev. Lett.* **96**, 110501 (2006).
- [14] H. de Riedmatten, I. Marcikic, J. A. W. van Houwelingen, W. Tittel, H. Zbinden, and N. Gisin, Long-distance entanglement swapping with photons from separated sources, *Phys. Rev. A* **71**, 050302(R) (2005).

- [15] M. Halder, A. Beveratos, N. Gisin, V. Scarani, C. Simon, and H. Zbinden, Entangling independent photons by time measurement, *Nat. Phys.* **3**, 692 (2007).
- [16] R. Kaltenbaek, R. Prevedel, M. Aspelmeyer, and A. Zeilinger, High-fidelity entanglement swapping with fully independent sources, *Phys. Rev. A* **79**, 040302(R) (2009).
- [17] C. Schmid, N. Kiesel, U. K. Weber, R. Ursin, A. Zeilinger, and H. Weinfurter, Quantum teleportation and entanglement swapping with linear optics logic gates, *New J. Phys.* **11**, 033008 (2009).
- [18] S. Takeda, M. Fuwa, P. van Loock, and A. Furusawa, Entanglement Swapping between Discrete and Continuous Variables, *Phys. Rev. Lett.* **114**, 100501 (2015).
- [19] B. P. Williams, R. J. Sadler, and T. S. Humble, Superdense Coding over Optical Fiber Links with Complete Bell-State Measurements, *Phys. Rev. Lett.* **118**, 050501 (2017).
- [20] G. Guccione, T. Darras, H. L. Jeannic, V. B. Verma, S. W. Nam, A. Cavallès, and J. Laurat, Connecting heterogeneous quantum networks by hybrid entanglement swapping, *Sci. Adv.* **6**, eaba4508 (2020).
- [21] S. Massar and S. Popescu, Optimal Extraction of Information from Finite Quantum Ensembles, *Phys. Rev. Lett.* **74**, 1259 (1995).
- [22] N. Gisin and S. Popescu, Spin Flips and Quantum Information for Antiparallel Spins, *Phys. Rev. Lett.* **83**, 432 (1999).
- [23] N. Gisin, Entanglement 25 years after quantum teleportation: Testing joint measurements in quantum networks, *Entropy* **21**, 325 (2019).
- [24] J. Czartowski and K. Życzkowski, Bipartite quantum measurements with optimal single-sided distinguishability, *Quantum* **5**, 442 (2021).
- [25] A. Tavakoli, N. Gisin, and C. Branciard, Bilocal Bell Inequalities Violated by the Quantum Elegant Joint Measurement, *Phys. Rev. Lett.* **126**, 220401 (2021).
- [26] A. Pozas-Kerstjens, N. Gisin, and A. Tavakoli, Full Network Nonlocality, *Phys. Rev. Lett.* **128**, 010403 (2022).
- [27] E. Bäumer, N. Gisin, and A. Tavakoli, Demonstrating the power of quantum computers, certification of highly entangled measurements and scalable quantum nonlocality, *npj Quantum Inf.* **7**, 117 (2021).
- [28] J.-F. Tang, Z. Hou, J. Shang, H. Zhu, G.-Y. Xiang, C.-F. Li, and G.-C. Guo, Experimental Optimal Orienteering via Parallel and Antiparallel Spins, *Phys. Rev. Lett.* **124**, 060502 (2020).
- [29] Z. Hou, J.-F. Tang, J. Shang, H. Zhu, J. Li, Y. Yuan, K.-D. Wu, G.-Y. Xiang, C.-F. Li, and G.-C. Guo, Deterministic realization of collective measurements via photonic quantum walks, *Nat. Commun.* **9**, 1 (2018).
- [30] C. Branciard, N. Gisin, and S. Pironio, Characterizing the Nonlocal Correlations Created via Entanglement Swapping, *Phys. Rev. Lett.* **104**, 170401 (2010).
- [31] C. Branciard, D. Rosset, N. Gisin, and S. Pironio, Bilocal versus nonbilocal correlations in entanglement-swapping experiments, *Phys. Rev. A* **85**, 032119 (2012).
- [32] M.-O. Renou, E. Bäumer, S. Boreiri, N. Brunner, N. Gisin, and S. Beigi, Genuine Quantum Nonlocality in the Triangle Network, *Phys. Rev. Lett.* **123**, 140401 (2019).
- [33] M. Weilenmann and R. Colbeck, Self-Testing of Physical Theories, or, is Quantum Theory Optimal with Respect to Some Information-Processing Task?, *Phys. Rev. Lett.* **125**, 060406 (2020).
- [34] R. Chaves, G. Moreno, E. Polino, D. Poderini, I. Agresti, A. Suprano, M. R. Barros, G. Carvacho, E. Wolfe, A. Canabarro, R. W. Spekkens, and F. Sciarrino, Causal networks and freedom of choice in Bell's theorem, *PRX Quantum* **2**, 040323 (2021).
- [35] M.-O. Renou, D. Trillo, M. Weilenmann, T. P. Le, A. Tavakoli, N. Gisin, A. Acín, and M. Navascués, Quantum theory based on real numbers can be experimentally falsified, *Nature (London)* **600**, 625 (2021).
- [36] See Supplemental Material at <http://link.aps.org/supplemental/10.1103/PhysRevLett.129.030502> for additional details on the setup and data analysis.
- [37] A. Tavakoli, M. O. Renou, N. Gisin, and N. Brunner, Correlations in star networks: From Bell inequalities to network inequalities, *New J. Phys.* **19**, 073003 (2017).
- [38] A. Tavakoli, P. Skrzypczyk, D. Cavalcanti, and A. Acín, Nonlocal correlations in the star-network configuration, *Phys. Rev. A* **90**, 062109 (2014).
- [39] N. Gisin, Q. Mei, A. Tavakoli, M. O. Renou, and N. Brunner, All entangled pure quantum states violate the bilocality inequality, *Phys. Rev. A* **96**, 020304(R) (2017).
- [40] F. Andreoli, G. Carvacho, L. Santodonato, R. Chaves, and F. Sciarrino, Maximal qubit violation of n -locality inequalities in a star-shaped quantum network, *New J. Phys.* **19**, 113020 (2017).
- [41] N. Lütkenhaus, J. Calsamiglia, and K.-A. Suominen, Bell measurements for teleportation, *Phys. Rev. A* **59**, 3295 (1999).
- [42] L. Vaidman and N. Yoran, Methods for reliable teleportation, *Phys. Rev. A* **59**, 116 (1999).
- [43] P. van Loock and N. Lütkenhaus, Simple criteria for the implementation of projective measurements with linear optics, *Phys. Rev. A* **69**, 012302 (2004).
- [44] X.-M. Hu, C.-X. Huang, Y.-B. Sheng, L. Zhou, B.-H. Liu, Y. Guo, C. Zhang, W.-B. Xing, Y.-F. Huang, C.-F. Li, and G.-C. Guo, Long-Distance Entanglement Purification for Quantum Communication, *Phys. Rev. Lett.* **126**, 010503 (2021).
- [45] C.-X. Huang, X.-M. Hu, B.-H. Liu, L. Zhou, Y.-B. Sheng, C.-F. Li, and G.-C. Guo, Experimental one-step deterministic polarization entanglement purification, *Sci. Bull.* **67**, 593 (2022).
- [46] X.-M. Hu, J.-S. Chen, B.-H. Liu, Y. Guo, Y.-F. Huang, Z.-Q. Zhou, Y.-J. Han, C.-F. Li, and G.-C. Guo, Experimental Test of Compatibility-Loophole-Free Contextuality with Spatially Separated Entangled Qutrits, *Phys. Rev. Lett.* **117**, 170403 (2016).
- [47] J. Fiurášek, Maximum-likelihood estimation of quantum measurement, *Phys. Rev. A* **64**, 024102 (2001).
- [48] X.-M. Hu, W.-B. Xing, B.-H. Liu, D.-Y. He, H. Cao, Y. Guo, C. Zhang, H. Zhang, Y.-F. Huang, C.-F. Li, and G.-C. Guo, Efficient distribution of high-dimensional entanglement through 11 km fiber, *Optica* **7**, 738 (2020).
- [49] V. Vedral, The role of relative entropy in quantum information theory, *Rev. Mod. Phys.* **74**, 197 (2002).
- [50] T. Kriváchy, Y. Cai, D. Cavalcanti, A. Tavakoli, N. Gisin, and N. Brunner, A neural network oracle for quantum nonlocality problems in networks, *npj Quantum Inf.* **6**, 70 (2020).